Supporting Information for

Tuning Nitrogen Species in 3D Porous Carbon via Boron doping for Boosted Zn-ion Storage Capability

Zhiran Zhang[a, b], Dandan Ouyang[a], Dongxu Chen [a, b], Liuqian Yang [a, b], Hui Zhu[a,b*], Jiao Yin[a,b*]

a Laboratory of Environmental Sciences and Technology, Xinjiang Technical Institute of Physics & Chemistry, Key Laboratory of Functional Materials and Devices for Special Environments, Chinese Academy of Sciences, Urumqi 830011, China

b Center of Materials Science and Optoelectronics Engineering, University of Chinese Academy of Sciences, Beijing 100049, China

Corresponding author: yinjiao@ms.xjb.ac.cn (J. Yin); huizhu@ms.xjb.ac.cn (H. Zhu)

Experimental Section:

Materials: The chemicals employed in this study include Sodium citrate (99%, Sigma-Aldrich), Potassium citrate (99%, Sigma-Aldrich), urea (99%, Sigma-Aldrich), boric acid (99%, Sigma-Aldrich) and hydrochloric acid (37%, Sigma-Aldrich). All the chemicals were used without further purification. Milli-Q ultrapure water with a resistivity of 18.2 MΩcm (25 °C) was used for all the experiments.

Material preparations: The B-doped rich edge-N porous carbon material was prepared by two-step method.

Step 1: 3 g potassium citrate, 7 g sodium citrate and 8 g urea were carbonized at 600 °C for 1 h under inert atmosphere with a temperature rate of 5 °C min^{-1}. The as obtained product was then washed with hydrochloric acid (1 M) and deionized water to remove the in situ generated template. Subsequently, the obtained product was dried in an oven at 80 °C for 12 h. To achieve uniform mixing, sodium citrate, potassium citrate and urea were dissolved in 100 mL deionized water and evaporated by stirring in a water bath at 80°C before calcination.

Step 2: 1 g carbon precursor prepared in the first step and different boric acid mass were heated at 800 °C for 1 h under inert atmosphere with a temperature rate of 5 °C min^{-1}. The products were washed several times with distilled water to remove the impurities and dried in an oven at 80 °C for 12h. Heteroatom doping carbon materials heated with different boric acid mass (2, 5 and 10 g) are denoted as $BENC_2$, $BENC_5$ and $BENC_{10}$, respectively. The preparation of NC was conducted according to the same procedure except adding boric acid.

Material characterizations:

The morphology features of samples were characterized by field-emission scanning electron microscopy (FESEM, JEOL JSM-7610FPLUS) and trans-mission electron microscope (TEM, FEI Tecnai G2 F20). The crystalline degree was analyzed by X-ray diffraction (XRD, Bruker D8 Advance Diffractometer) and Raman spectra were obtained on a Labram HR Raman Evolution spectrometer with the incident light wavelength of 532 nm. The specific surface area and porosity were determined by 77 K N adsorption/desorption isotherm (ASAP2020, Micromeritics, USA). Surface characteristics of as prepared carbons were obtained by the X-ray photoelectron spectrum (XPS) on the ESCALAB 250 (Thermo Electron) in which the excitation of X-ray resource was provided by a monochromatic source of Al Kα. TR (Transmission) test mode was used for Fourier transform infrared spectroscopy (FTIR, Thermofisher Nicolet IS50) measurement to collect the chemical information of the sample. The EPR spectroscopy of samples were characterized by Bruker ELEXSYS-II E500 CW-EPR, Germany.

Electrochemical properties:

The electrochemical measurements of carbon samples were carried out by using a thin film electrode. The carbon film electrode was made by mixing the active material (BENC), PVDF binder and Super-P carbon with a mass ratio of 7:2:1. The mass loading of the active material was about 1.0 mg $cm^{-2.}$ The carbon film is then pressed on the stainless steel current collector with a pressure of 1 MPa. Zinc-ion hybrid capacitors (ZIHCs) were assembled in cion cells using 2M $ZnSO_4$ aqueous solution as the

electrolyte, zinc foil as the anode, the as-obtained materials as the cathode and glass microfiber as the separator. The quasi-solid-state ZHICs were prepared by zinc foil, carbon cathode and acrylamide/$ZnSO_4$ gel. Preparation of acrylamide/$ZnSO_4$ gel :1.5 g acrylamide, 7 mg potassium persulfate and 1 mg methylene-bis-acrylamide were added to 2 M $ZnSO_4$ solution, then the gel was poured into the mold (80* 60* 10 mm) and kept at 60 ° C for 3h.

Electrochemical measurement:

Galvanostatic charge/discharge (GCD) curves were recorded on the Land system (Land, Wuhan). Cyclic voltammetry (CV) and electrochemical impedance spectroscopy (EIS) were performed on electrochemical workstation (CHI760, Chenhua, Shanghai).

The specific capacitance of ZIHCs was calculated as follows:

$$C = \frac{I \times \Delta t}{m \times \Delta V} \quad (1)$$

where C (F g^{-1}) is the specific capacitance, I (A) is the discharge current, Δt (s) is the discharge time, ΔV (V) is the working voltage window of ZIHC, namely 0.2-1.8 V, m (g) corresponds to the quality of the active material in the electrode.

Use the following formulas to calculate the energy density E_t (Wh kg^{-1}) and power density P_t (W kg^{-1}) of ZIHCs:

$$E_t = \frac{1}{2} \times C \times \Delta V^2 \times \frac{1}{3.6} \quad (2)$$

$$P_t = \frac{E}{\Delta t} \times 3600 \quad (3)$$

Where E_t (Wh kg^{-1}) and P_t (W kg^{-1}) are the energy density and power density of the ZIHCs, respectively, Δt (s) is the charge time, ΔV (V) is the working voltage window of ZIHCs, C is the device capacitance.

Density Functional Theory Simulation:

A prototype model based on the graphene structure of 8× 8 unit cells was constructed and its basic trend was explained. The defect was carved by removing carbon atoms, with the edges saturated with hydrogen atoms. The structural optimization was performed at the revised Perdew-Burke-Ernzerhof (rPBE) (PRL, 1998, 80, 890) level of density functional theory (DFT) calculations. The electrons were described by the augmented plane wave (PAW) method (PRB, 1994, 50, 17953) with an energy cutoff of 400 eV. The energy convergence criterial was set to be 1 ~ 6 eV. The binding energy was calculated through $E_b = E_{total} - E_{sheet} – E_{Zn}$.

Supplementary Figures and Tables

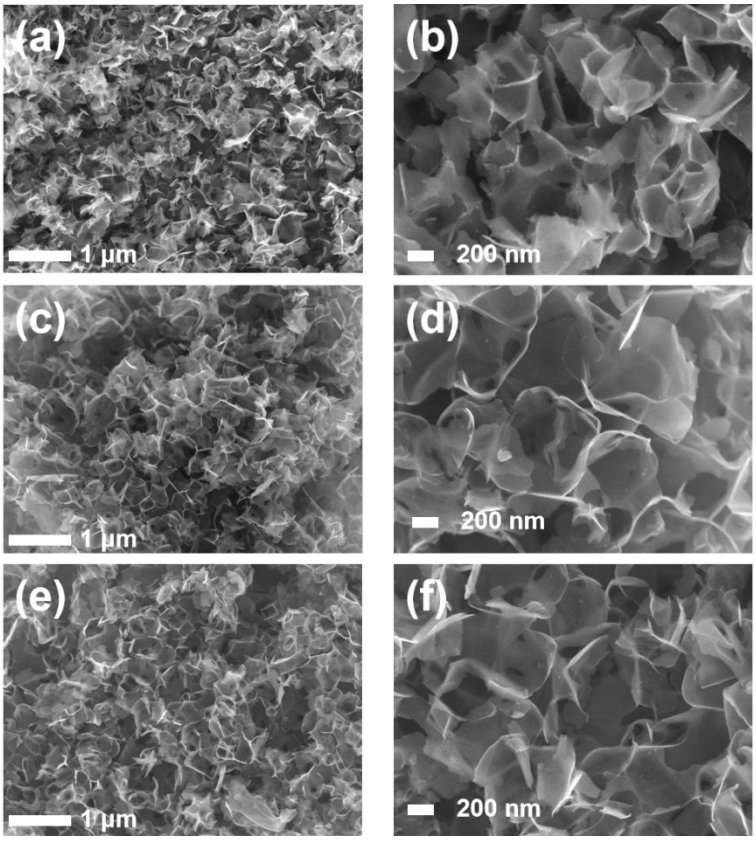

Fig. S1 SEM images with different magnification of (a, b) NC, (c, d) $BENC_2$, and (e, f) $BENC_{10}$

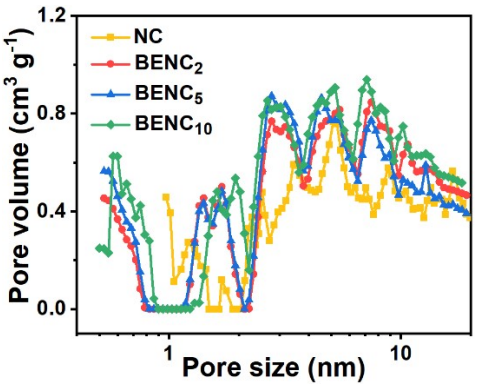

Fig. S2 Pore size distribution curves of samples.

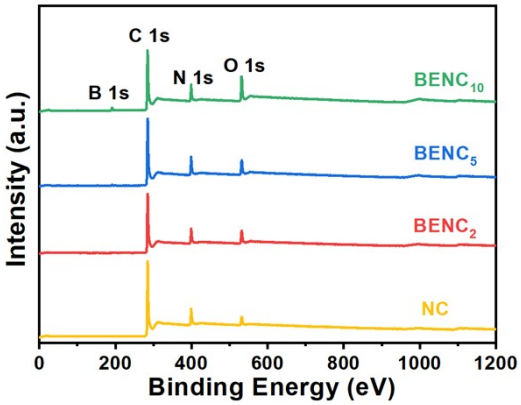

Fig. S3 XPS spectra of samples.

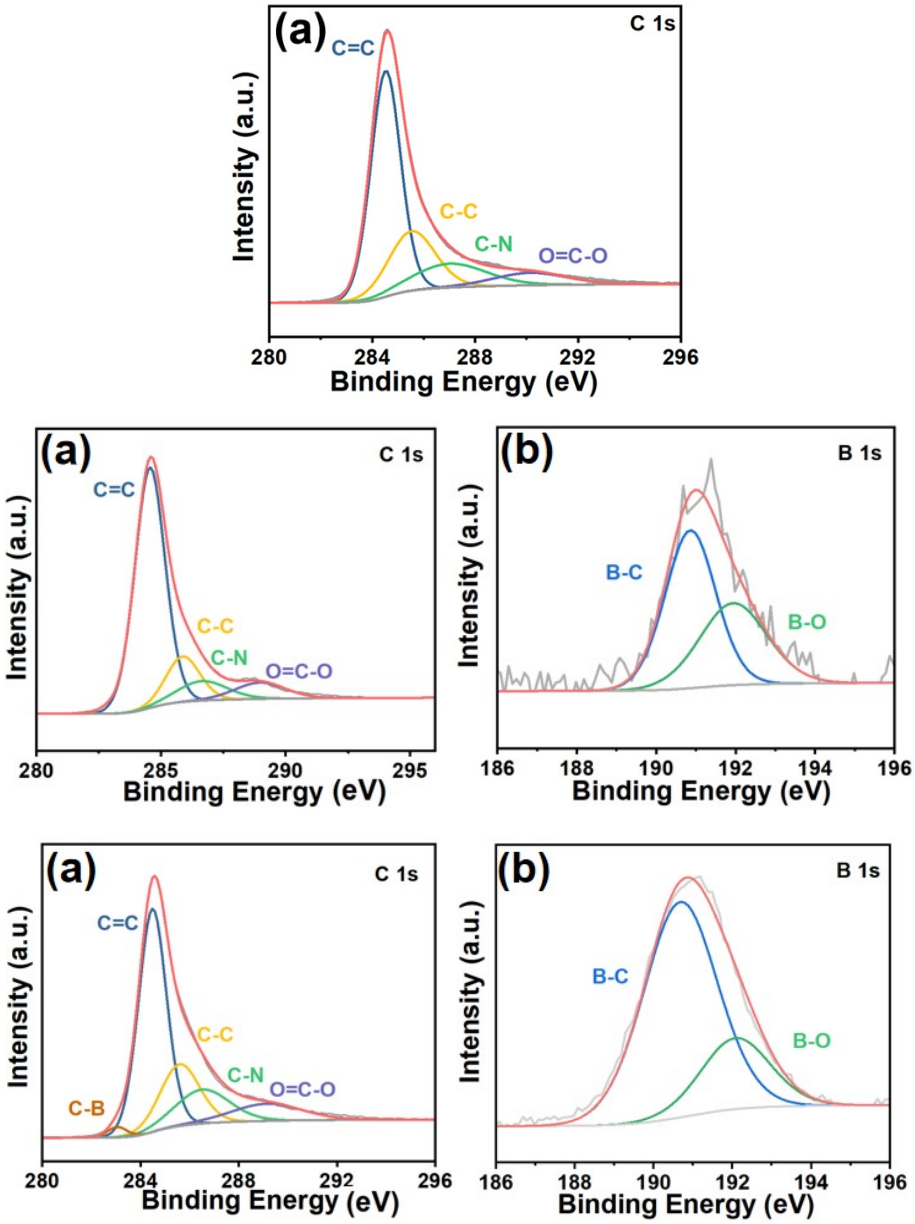

Fig. S4 High-resolution C 1s XPS spectra of (a) NC, (b) $BENC_2$, (d) $BENC_{10}$ and B 1s XPS spectra of (c) $BENC_2$, (e) $BENC_{10}$.

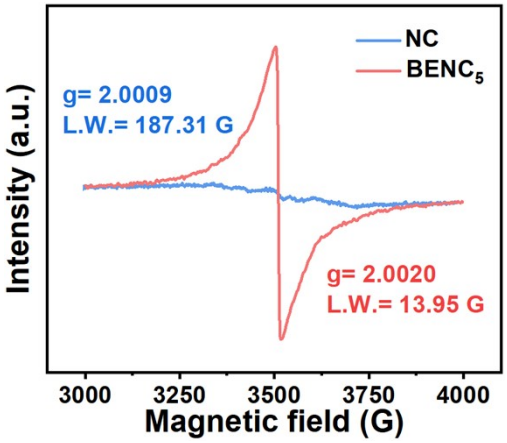

Fig. S5 EPR spectra of the NC and the $BENC_5$, respectively.

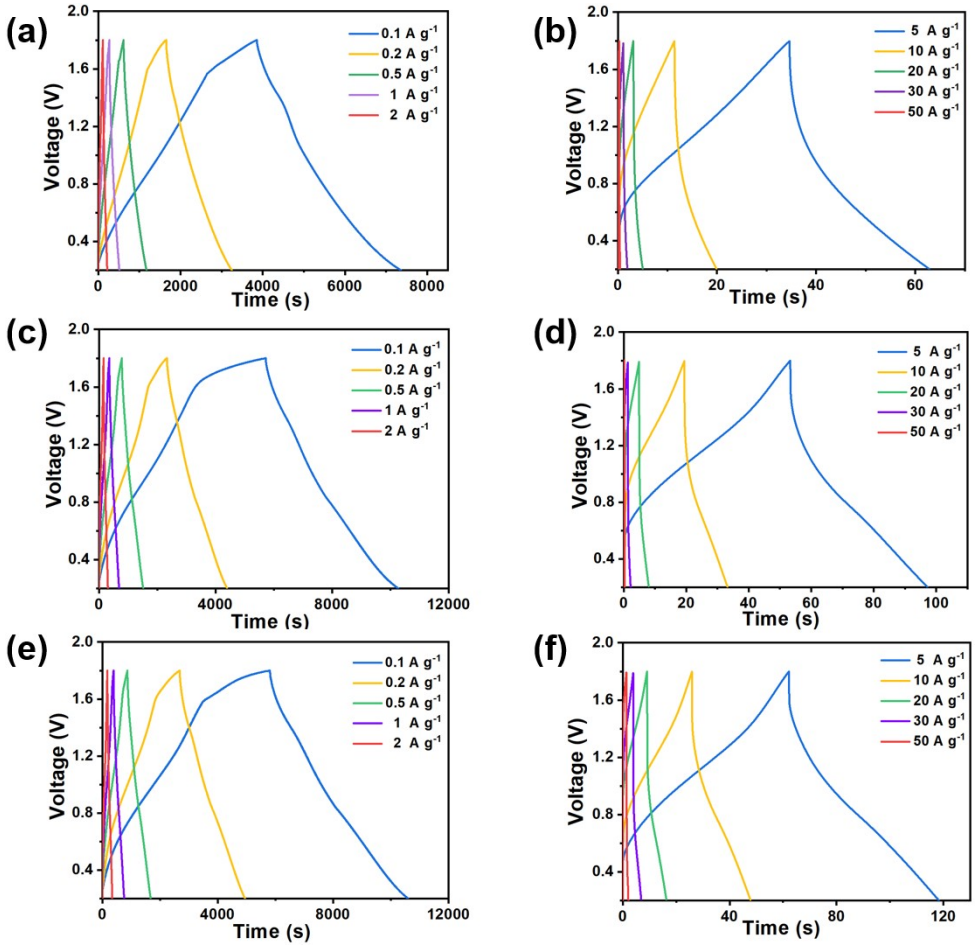

Fig. S6 GCD curves of (a, b) Zn//NC ZIHC, (c, d) Zn//$BENC_2$ ZIHC and (e, f) Zn//$BENC_{10}$ ZIHC at various current densities.

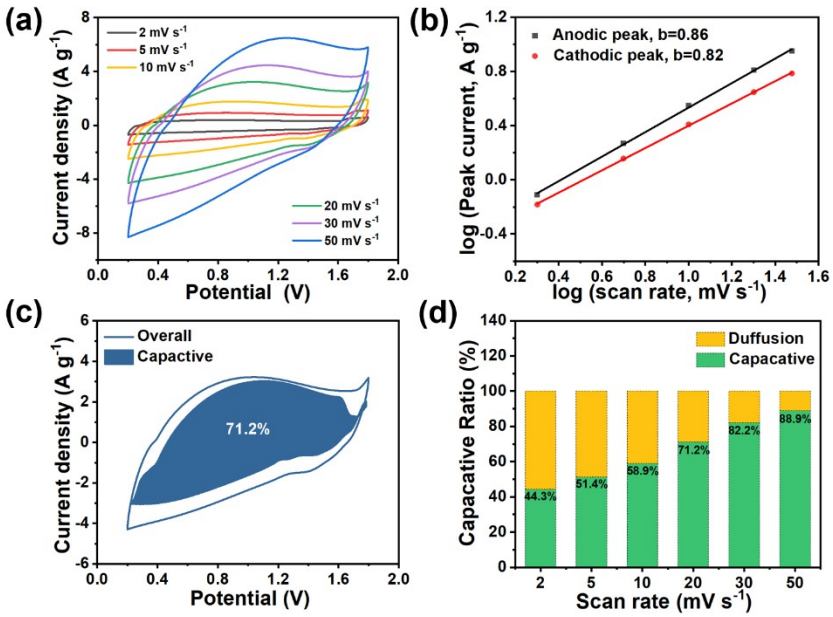

Fig. S7 (a) CV curves of Zn//NC ZIHC at various scan rates from 2 to 50 mV s^{-1}. (b) Linear relationships between logarithm currents and logarithm sweep rates. (c) Reaction kinetics contribution at 20 mV s^{-1} of NC cathode. (d) Normalized contribution ratio of ultrarapid reaction kinetics-controlled processes at various scan rates.

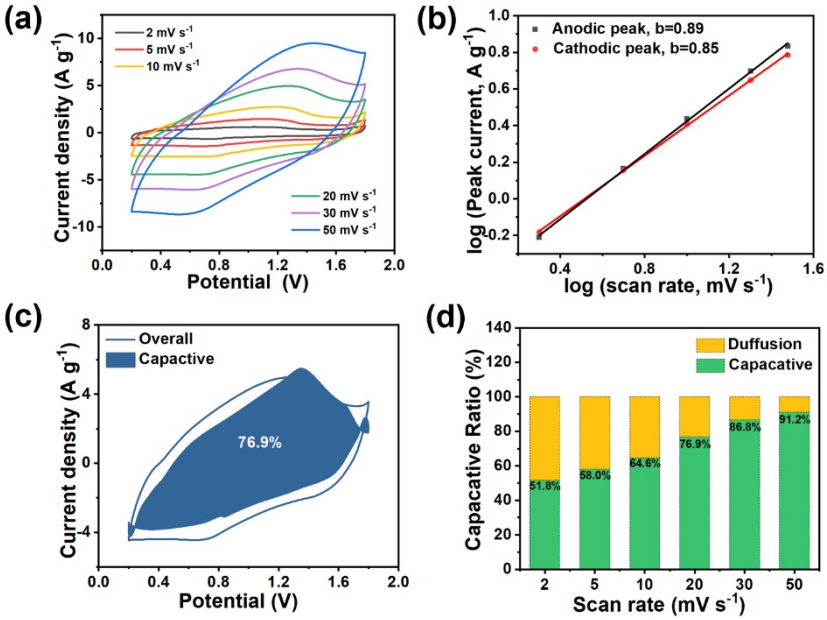

Fig. S8 (a) CV curves of Zn//$BENC_2$ ZIHC at various scan rates from 2 to 50 mV s^{-1}. (b) Linear relationships between logarithm currents and logarithm sweep rates. (c) Reaction kinetics contribution at 20 mV s^{-1} of $BENC_2$ cathode. (d) Normalized contribution ratio of ultrarapid reaction kinetics-controlled processes at various scan rates.

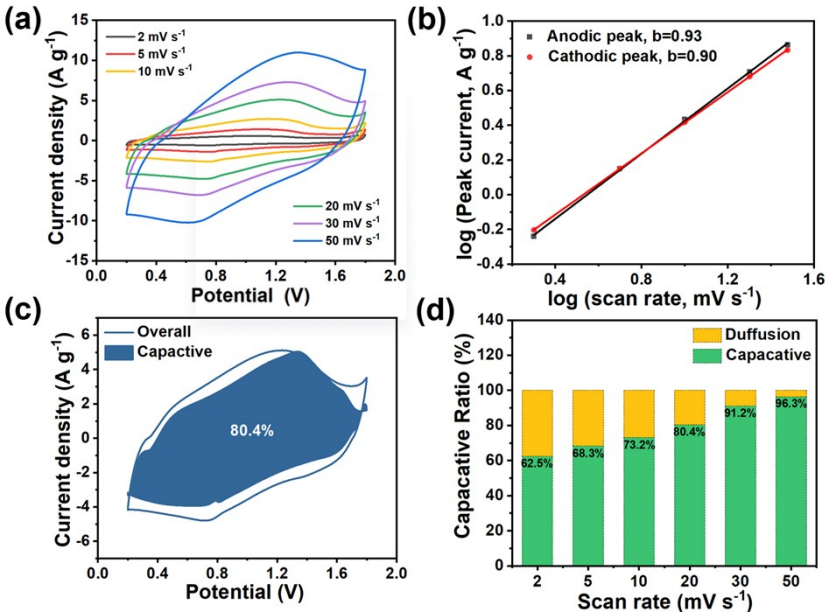

Fig. S9 (a) CV curves of Zn//BENC$_{10}$ ZIHC at various scan rates from 2 to 50 mV s^{-1}. (b) Linear relationships between logarithm currents and logarithm sweep rates. (c) Reaction kinetics contribution at 20 mV s^{-1} of BENC$_{10}$ cathode. (d) Normalized contribution ratio of ultrarapid reaction kinetics-controlled processes at various scan rates.

Table S1. Porosity parameters of NC and BENCs.

Samples	S_{BET} /m^2 g^{-1}	S_{micro} /m^2 g^{-1}	V_{total} /cm^3 g^{-1}	V_{micro} /cm^3 g^{-1}	S_{micro}/S_{BET} %	S_{meso}/S_{BET} %
NC	560	123	0.63	0.05	21.9	78.1
$BENC_2$	665	131	0.79	0.05	19.7	80.3
$BENC_5$	732	143	0.75	0.06	19.5	80.5
$BENC_{10}$	771	198	0.80	0.06	25.7	74.3

Table S2. Elemental analysis (according to XPS) of NC and BENCs.

Samples	C (at%)	N (at%)	B (at%)	O (at%)
NC	88.70	7.95	-	3.35
$BENC_2$	84.12	9.00	2.56	4.32
$BENC_5$	81.33	8.86	4.62	5.19
$BENC_{10}$	72.04	8.39	11.34	8.23

Table S3. Nitrogen species analysis (according to XPS) of NC and BENCs.

Samples	N-5 (at%)	N-6 (at%)	N-Q (at%)	N-O (at%)
NC	21.0	40.6	27.4	11.0
$BENC_2$	37.2	34.9	18.6	9.3
$BENC_5$	35.4	46.2	12.5	5.9
$BENC_{10}$	32.6	49.5	10.8	7.1

Table S4. Nitrogen species analysis (according to XPS) of NC and BENCs.

Samples	Rs (Ω)	Rct (Ω)
$BENC_5$	0.81	109.9
$BENC_{10}$	1.1	213.4

Table S5. Zn^{2+} storage performance of $BENC_5$ compared with previously reported materials.

Materials	Electrolyte	Voltage range (V)	Capacity	Current Density ($A\ g^{-1}$)	Electrochemical performance	Ref.
AC	2 M $ZnSO_4$	0.2-1.8	121 mA h g^{-1}	0.1	91% after 10,000 cycles	1
AC	1 M $Zn(CF_3SO_3)_2$	0-1.7	170 F g^{-1}	0.1	91% after 20,000 cycles	2
PSC-A600	1 M $Zn(CF_3SO_3)_2$	0.2-1.8	183.7 mA h g^{-1}	0.2	92.2% after 10,000 cycles	3
MSAC	1 M $ZnSO_4$	0.3-1.8	176 mA h g^{-1}	0.5	78% after 40,000 cycles	4
PCN	1 M $ZnSO_4$	0.1-1.7	149 mA h g^{-1}	0.2	91% after 10,000 cycles	5
MPC	1 M $Zn(CF_3SO_3)_2$	0-1.8	209 F g^{-1}	0.2	100% after 10,000 cycles	6
HCSs	2 M $ZnSO_4$	0.15-1.95	86.8 mA h g^{-1}	0.5	98% after 15,000 cycles	7
B/N co-doped LDC	1 M $ZnSO_4$	0.2-1.8	127.7 mA h g^{-1}	0.5	/	8
N-HPC	2 M $ZnSO_4$	0.2-1.8	136.8 mA h g^{-1}	0.5	90.9% after 5000 cycles	9

B-diamond/ carbon fiber	1 M $ZnSO_4$	0.2-1.8	35.1 F g^{-1}	0.2	89.9% after 10,000 cycles	10
LNPC	1 M $ZnSO_4$	0.2-1.8	266 F g^{-1}	0.05	/	11
LPCS	1 M $ZnSO_4$	0.2-1.8	301 F g^{-1}	0.1	95% after 5000 cycles	12
TCNTs	2 M $ZnSO_4$	0.2-1.8	240.4 F g^{-1}	0.1	100% after 10,000 cycles	13
NPFC	1 M $Zn(CF_3SO_3)_2$	0.2-1.8	207.9 F g^{-1}	0.1	97.4% after 20,000 cycles	
$BENC_5$	2 M $ZnSO_4$	0.2-1.8	354.6 F g^{-1} /157.5 mA h g^{-1}	0.1	99.1% after 20,000 cycles	This work

Reference

1 L. Dong, X. Ma, Y. Li, L. Zhao, W. Liu, J. Cheng, C. Xu, B. Li, Q.-H. Yang, F. Kang, *Energy Storage Materials*,2018, **13,** 96-102.

2 H. Wang, M. Wang, Y. Tang, *Energy Storage Materials*,2018, **13,** 1-7.

3 Z. Li, D. Chen, Y. An, C. Chen, L. Wu, Z. Chen, Y. Sun, X. Zhang, *Energy Storage Materials*,2020, **28,** 307-314.

4 G.-H. An, *Applied Surface Science*,2020, **530,** 147220.

5 D. Wang, Z. Pan, Z. Lu, *Microporous and Mesoporous Materials*,2020, **306,** 110445.

6 C. Jiang, Z. Zou, *Diamond and Related Materials*,2020, **101,** 107603.

7 S. Chen, L. Ma, K. Zhang, M. Kamruzzaman, C. Zhi, J.A. Zapien, *Journal of Materials Chemistry A*,2019, **7,** 7784-7790.

8 Y. Lu, Z. Li, Z. Bai, H. Mi, C. Ji, H. Pang, C. Yu, J. Qiu, *Nano Energy*,2019, **66,** 104132.

9 P. Liu, Y. Gao, Y. Tan, W. Liu, Y. Huang, J. Yan, K. Liu, *Nano Research*,2019, **12,** 2835-2841.

10 Z. Jian, N. Yang, M. Vogel, S. Leith, A. Schulte, H. Schönherr, T. Jiao, W. Zhang, J. Müller, B. Butz, X. Jiang, *Advanced Energy Materials*,2020, **10,** 2002202.

11 W. Zhang, J. Yin, W. Jian, Y. Wu, L. Chen, M. Sun, U. Schwingenschlögl, X. Qiu, H.N. Alshareef, *Nano Energy*,2022, **103,** 107827.

12 F. Wen, Y. Yan, S. Sun, X. Li, X. He, Q. Meng, J. Zhe Liu, X. Qiu, W. Zhang, *J Colloid Interface Sci*,2023, **640,** 1029-1039.

13 S. Yan, Y. Tang, L. Liu, Y. Gao, Y. Zhang, C. Yang, *ACS Applied Energy Materials*,2023, **6,** 4144-4149.

14 F. Wei, Y. Wei, J. Wang, M. Han, Y. Lv, *Chemical Engineering Journal*,2022, **450,** 137919.